Shape transition in Os and Pt isotopes

A. Ansari*
International Centre for Theoretical Physics, 34100 Trieste, Italy
(Received 26 August 1985)

Ground state structure of the $A=186-196$ Os-Pt region is investigated through a self-consistent Hartree-Fock-Bogoliubov calculation employing a pairing plus quadrupole plus hexadecapole model interaction Hamiltonian. The influence of the hexadecapole degrees of freedom on the triaxiality is especially examined. A gradual prolate to oblate shape transition is found in Pt isotopes but such a change is almost abrupt in Os at $A\approx 194$. This difference in behavior of the Os and Pt isotopes is obtained only if all the hexadecapole degrees of freedom, instead of merely an axial Y_{40} component, are treated fully self-consistently.

I. INTRODUCTION

By now there exists an exhaustive list of theoretical as well as experimental papers devoted to the study of the structure of the complex transitional Os-Pt region. Of particular interest is the change of the quadrupole deformation parameter β_2 and asymmetry parameter γ as a function of the mass number A for the Os and Pt nuclei. Recent empirical results[1,2] indicate that the prolate ($\gamma=0°$) to oblate ($\gamma=60°$) shape transition, in going from lighter to heavier isotopes, takes place quite gradually in Pt isotopes, whereas in Os it occurs almost suddenly at $A\approx 192-194$. Our main motivation here is to throw some light on the understanding of this dissimilar behavior of the Os and Pt isotopes in the mass region $A=186-196$.

But before going into details of our present work we would like to mention briefly some of the relevant work already done. The microscopic and semimicroscopic approaches[3-10] usually lead to γ-soft or γ-unstable[11] ground state intrinsic shapes of these nuclei, which means that the energy minima are very shallow in the γ space. On the other hand, various γ-rigid models[12-16] have had good success in reproducing the experimental data on low lying excitation energies and $B(E2)$ transition rates. However, now the experimental data are so exhaustive that the weak points of the theoretical models cannot go unnoticed. For instance, the γ-rigid models do fail to reproduce well the $B(E2;\gamma\rightarrow\text{g.s.})$ transitions.

In recent years more productive have been the so-called IBM-1 and IBM-2 interacting boson model approaches[17-22] to describe the collective properties of the transitional nuclei. It is a well-known fact that the nuclear deformation is caused by the n-p interaction amongst the valence nucleons of a nucleus.[23,24] In this sense the IBM-2 version has the right ingredients and has been applied very successfully to interpret the data in the Os-Pt region. Very recently, Casten[25] has attempted to present a unified model to study the change of nuclear deformation (essentially the excitation energy ratio E_4/E_2) as a function of A in terms of the product of the valence number of protons and neutrons in a nucleus. Stuchbery[26,27] finds that even IBM-2 is not able to explain simultaneously the energy spectrum, $B(E2)$ transition rates, and g-factors as a function of spin as well as the mass number. Thus study of the intrinsic structure of the transitional region is still an interesting and challenging problem.

Now coming back to the triaxial shapes of the transitional nuclei, in 1972 Götz *et al.*[7] had shown in a detailed Strutinsky calculation[28] that inclusion of the hexadecapole (β_4) degree of freedom is very essential to get the oblate shape at a correct mass number. Ragnarsson *et al.*[8] have shown that the prolate shape gets lowered in energy compared to the oblate shape if a β_4 deformation term is included in the Hamiltonian. Baker *et al.*[15-29] have shown from the analysis of their data that heavy transitional Os and Pt nuclei do possess nonzero (small) negative hexadecapole deformations and the γ and β_4 degrees of freedom cannot be separated from each other. However, we must emphasize that, for the reasons of numerical simplicity, so far in all the theoretical studies[7,8,30-33] only a $\beta_4 r^2 Y_{40}$ term or a somewhat generalized form of this term is included such that it is always operative along any axis of symmetry (X, Y, or Z corresponding to which γ is 120°, 60°, or 0°, respectively). For a general intermediate value of γ it is some admixture of various $Y_{4\mu}$ terms. Soon, in the next section, we shall elaborate more on this. Thus, actually for a triaxial nucleus (say, $\gamma=20°-40°$) it may be essential to treat the hexadecapole degrees of freedom in a more realistic way. With this aim we have performed a self-consistent Hartree-Fock-Bogoliubov (HFB) calculation[3,4] to study the ground state intrinsic shapes of the Os-Pt nuclei adding a hexadecapole interaction term to the pairing plus quadrupole model Hamiltonian of Baranger and Kumar (BK) (Ref. 3) and find some interesting results.

In Sec. II we outline the calculational scheme, and we present our results and discussions in Sec. III. Finally the conclusions of the present study are summarized in Sec. IV.

II. CALCULATIONAL SCHEME

As mentioned in the previous section, the Hamiltonian used is essentially the pairing plus quadrupole model interaction of BK (Ref. 3) with an extra hexadecapole term added to it

$$H=\sum_{\tau,\alpha}\epsilon_\alpha^\tau C_\alpha^\dagger C_\alpha-\tfrac{1}{2}\sum_{\lambda=2,4}\chi_\lambda\sum_{\substack{\alpha,\beta,\gamma,\delta\\ \mu,\sigma,\tau}}\alpha_\sigma\alpha_\tau\langle\alpha\,|\,Q_{\lambda\mu}^\sigma\,|\,\gamma\rangle\langle\beta\,|\,Q_{\lambda\mu}^{\dagger\tau}\,|\,\delta\rangle C_\alpha^\dagger C_\beta^\dagger C_\delta C_\gamma-\tfrac{1}{4}\sum_\tau G_\tau\sum_{\alpha,\gamma}C_\alpha^\dagger C_{\bar\alpha}^\dagger C_{\bar\gamma}C_\gamma\ . \tag{1}$$

Various symbols have the same meaning as in Ref. 3, viz., χ_λ is the multipole interaction strength and G_τ the pairing interaction strength with σ,τ=proton or neutron and

$$Q_{\lambda\mu}=r^2Y_{\lambda\mu}(\theta,\phi)\ . \tag{2}$$

The basis space and spherical single-particle (sp) energies are precisely that of BK.[3]

The expectation value of the above Hamiltonian (1) is minimized with respect to the relevant shape parameters of the Bardeen-Cooper-Schrieffer–type (BCS) intrinsic many-body wave function

$$\Phi=\prod_i(U_i+V_ia_i^\dagger a_{\bar i}^\dagger)\,|\,0\rangle\ , \tag{3}$$

where $a_i^\dagger$ creates a particle in the deformed Nilsson orbital

$$|\,i\rangle=\sum_\alpha C_\alpha^i\,|\,\alpha\rangle \tag{4}$$

and $a_{\bar i}^\dagger$ does so in the corresponding time reversed orbital. V_i and U_i are obviously the BCS transformation amplitudes for the occupation and emptiness of an orbital $|\,i\rangle$.

Then the main task is to carry out the energy minimization calculation in three types of numerical schemes:

($S1$): Standard self-consistent HFB calculation of BK (Ref. 3) with

$$\chi_2=70/A^{1.4}\ ,\quad \chi_4=0.0\ ,$$
$$G_p=27/A\ ,\quad G_n=22/A \tag{5}$$

(all in MeV). For all the nuclei considered here, except ^{194,196}Os, results can be directly taken from Ref. 3.

($S2$): Besides β_2 and γ which are present in the BK many-body wave function, an axial hexadecapole deformation parameter β_4 is also included in the wave function. Usually it is simply introduced through the use of a Nilsson-type deformed one-body Hamiltonian

$$h=h_s-\hbar\omega\beta_2\left[\cos\gamma Q_{20}+\frac{1}{\sqrt{2}}\sin\gamma(Q_{22}+Q_{2-2})\right]$$
$$-\hbar\omega\beta_4Q_{40}\ , \tag{6}$$

where h_s stands for the spherical sp part and $\hbar\omega=41.2/A^{1/3}$ is the oscillator frequency. However, this form of the β_4 term is correct only for $\gamma=0°$ or 180°. In recent years, as already mentioned, it has been somewhat generalized[30,31] in such a way that for any axis of symmetry ($\gamma=0°$, Z axis; $\gamma=60°$, Y axis; $\gamma=120°$, X axis) we have always a corresponding Q_{40} term operative, and for any other γ values some combination of $Y_{40}(\hat X)$, $Y_{40}(\hat Y)$, and $Y_{40}(\hat Z)$ is present. Thus in this scheme (6) is replaced by

$$h=h_s-\hbar\omega\beta_2\left[\cos\gamma Q_{20}+\frac{1}{\sqrt{2}}\sin\gamma(Q_{22}+Q_{2-2})\right]$$
$$-\hbar\omega\beta_4[C_X(\gamma)Q_{40}(\hat X)+C_Y(\gamma)Q_{40}(\hat Y)+C_Z(\gamma)Q_{40}(\hat Z)], \tag{7}$$

where the forms of the coefficients $C(\gamma)$ guarantee the above-mentioned properties. We use the one proposed in Ref. 30. Thus in this scheme of calculation we have three free parameters, β_2, γ, and β_4, besides the pairing gap parameters Δ_p and Δ_n for protons and neutrons, respectively.

($S3$): Treat all the components of the hexadecapole force self-consistently to minimize the energy. One straightforward way, which we have adopted here, is to perform a self-consistent HFB calculation with the general Hamiltonian of Eq. (1) with $\chi_4\neq0$. In this case neglecting in the manner of Baranger and Kumar[3] the exchange matrix elements, the one-body Hamiltonian corresponding to the hexadecapole term will look like

$$h_4=\sum_\mu D_{4\mu}Q_{4\mu}\ ;\quad \mu=-4,-2,0,2,4$$

with

$$D_{4\mu}=\chi_4\sum_\tau\langle Q_{4\mu}^\tau\rangle=(-1)^\mu D_{4-\mu}\ . \tag{8}$$

We may define β_4 through the relation

$$\hbar\omega\beta_4=D_{40}\ . \tag{9}$$

It is obvious that now we have five deformation parameters, β_2, γ, β_4, D_{42}, and D_{44}. However, in a self-consistent iterative calculation the computing time is comparable to the case when only the first three parameters are considered as free.

In the case of schemes $S2$ and $S3$ the interaction strengths in Hamiltonian (1) are taken as

$$\chi_2=\chi_4=70/A^{1.4}\ ,\quad G_p=28/A\ ,\quad G_n=23/A\ . \tag{10}$$

Several values, including $\chi_2\neq\chi_4$ in the neighborhood of BK values, Eq. (5), have been tried but these seem to be good enough to reproduce approximately the pairing gap parameters and β_2 of BK.[3] It should be clear that $S1$ and $S3$ differ only in the choice of the Hamiltonian, i.e., the interaction strengths (5) and (10). On the other hand, $S2$ and $S3$ utilize the same Hamiltonian to calculate the energy but differ in the choice of the many-body trial wave function for the variational calculation.

III. RESULTS AND DISCUSSIONS

Our main concern here is to investigate the effect of the hexadecapole degrees of freedom on the value of γ as a function of A in the transitional region with an additional motive to ascertain the extent of the usefulness of expression (7). We must emphasize that the present attempt is

still only a model calculation. The basis space is restricted only to two major shells $N=4,5$ for protons and $N=5,6$ for neutrons. The values of interaction strength parameters (10) are also, perhaps, not very unique though rather close to the BK values (5).

A. Self-consistent intrinsic results

Through the minimization of energy as a function of various shape parameters we determine their equilibrium values in the three schemes of calculation $S1$, $S2$, and $S3$, for $A=186$–196. Our results for the shape parameter β_2, γ, β_4, and the pairing gaps (in MeV) Δ_p and Δ_n are listed in Table I for the nuclei considered here. The three rows of numbers for each isotope correspond to the schemes $S1$, $S2$, and $S3$, respectively. From the ground band experimental spectrum[1,2,29,34–39] the ratio E_4/E_2 is also enumerated to be compared with the ideal rotor value of 3.33 and the vibrator limit of 2.0. We notice that for the Pt isotopes considered here this is almost a constant 2.5, whereas for Os it reaches this value only at $A=196$. We should remind that in $S3$ we have actually three independent hexadecapole parameters $D_{4\mu}$, but for the comparison we have listed only β_4 calculated from D_{40} using the relation (9).

As pointed out long ago by Ragnarsson *et al.*,[8] the effect of the β_4 term is to favor the prolate shape compared to the oblate one. We too find the tendency of γ decreasing in the presence of hexadecapole terms, and the larger the value of β_4 the bigger is the effect. Considering only the quadrupole force, BK (Ref. 3) found that osmium isotopes exhibit prolate to oblate shape transition from $A=186$ to 192 somewhat gradually in comparison to Pt (see the first rows of Table I). Whereas our results corresponding to $S3$ show an opposite behavior which seems to agree with the present understanding based on the analysis of the experimental results (for instance see Ref. 2), particularly the decay pattern of several excited 0^+ states to the ground band 2^+ state. We should further add that for ^{192}Os we also get a prolate ($\gamma=0$) minimum with $\beta_2=0.145$ and $\beta_4=-0.045$ which is higher compared to the absolute minimum at $\gamma=46°$ only by about 75 keV. Thus these two minima would compete with each other to describe the physical ground state. In their Strutinsky[28] calculation including a β_4 term Gotz *et al.*[7] predicted Os nuclei with competing prolate and oblate axial shapes. Here the $S2$ approach seems to be good enough to predict a rapid prolate to oblate structural phase transition in Os isotopes. Nevertheless, to produce a gradual shape change in Pt isotopes $S3$ seems to be essential. The most significant difference between the $S2$ and $S3$ schemes is seen in the case of ^{190}Pt and ^{192}Pt out of all the nuclei considered here.

B. Potential energy surface plots

The values of the shape parameters presented in Table I correspond to the energy minima. But at the same time a study of the variation of energy in the full parameter space is often very useful. However, we have three free parameters in the $S2$ approach and five in the $S3$ approach. From Table I we notice that $\beta_4(S3)\geq\beta_4(S2)$,

TABLE I. Self-consistent intrinsic results for Os and Pt isotopes with mass numbers $A=186$–196. For every A three rows correspond to the three schemes of calculation, $S1$, $S2$, and $S3$, respectively. For prolate shapes ($\gamma=0$) the second and third rows become identical. As an experimental measure of deformation the ground band energy ratio $E4/E2$ is also listed.

	^{76}Os						^{78}Pt					
A	β_2	$\gamma^{[0]}$	β_4	Δ_p	Δ_n	E_4/E_2[a]	β_2	$\gamma^{[0]}$	β_4	Δ_p	Δ_n	E_4/E_2[a]
186	0.199	0.0	0.0	0.760	0.970	3.17	0.188	0.0	0.0	0.722	0.984	2.56
	0.214	0.0	−0.052	0.738	0.935		0.194	0.2	−0.031	0.784	1.036	
	0.214	0.0	−0.052	0.738	0.935		0.194	0.2	−0.031	0.784	1.036	
188	0.180	21.4	0.0	0.790	0.993	3.08	0.170	20.2	0.0	0.672	1.050	2.53
	0.196	0.0	−0.055	0.729	0.970		0.178	7.6	−0.035	0.744	1.077	
	0.196	0.0	−0.055	0.729	0.970		0.178	6.8	−0.035	0.747	1.071	
190	0.170	49.5	0.0	0.834	0.994	2.93	0.155	60.0	0.0	0.682	1.092	2.49
	0.172	0.0	−0.052	0.759	0.977		0.157	40.0	−0.013	0.724	1.166	
	0.172	0.0	−0.052	0.759	0.977		0.159	25.8	−0.026	0.706	1.122	
192	0.152	60.0	0.0	0.851	0.935	2.82	0.144	60.0	0.0	0.681	1.038	2.48
	0.151	54.8	−0.006	0.919	1.036		0.144	53.0	−0.006	0.740	1.137	
	0.155	46.3	−0.017	0.897	1.003		0.147	45.4	−0.014	0.722	1.109	
194	0.143	60.0	0.0	0.849	0.789	2.75	0.134	60.0	0.0	0.681	0.951	2.47
	0.137	58.4	−0.004	0.925	0.912		0.132	57.4	−0.004	0.743	1.056	
	0.138	55.7	−0.008	0.920	0.910		0.134	53.4	−0.009	0.734	1.047	
196	0.125	60.0	0.0	0.861	0.629	2.53	0.125	60.0	0.0	0.680	0.817	2.47
	0.113	58.5	−0.004	0.943	0.803		0.119	58.6	−0.004	0.748	0.940	
	0.115	56.0	−0.009	0.939	0.803		0.121	56.3	−0.007	0.742	0.938	

[a]Data taken from Refs. 1, 2, 29, and 34–36 for Os and Refs. 37–39 for Pt isotopes.

whereas $\beta_4(S1)=0$. So, we have drawn potential energy surface (PES) contour plots in the (β_2,γ) space for a fixed value of β_4 calculating energy only in the scheme $S2$. The effect of $S3$ is reflected only qualitatively through the use of a larger β_4. In the figures, the top right corner of each plot $S1$, $S2$, or $S3$ indicates that the β_4 value used there corresponds to the equilibrium value in that scheme. The contour lines labeled $A,B,\ldots,J$ correspond to 20, 50, 100, 150, 250, 800, 1000, 1250, and 1500 keV energies, respectively, on each figure. This separation is rather arbitrarily adopted to have a better disposition near the minimum. Instead of all the nuclei considered here we have chosen only some typical interesting cases, namely ^{190,192,194}Os and ^{188,190}Pt.

Figure 1(a) shows that for ^{190}Os BK predict almost an oblate shape with $\gamma\approx 35°-60°$ within an energy spread of $|\Delta E|=20$ keV. But with the inclusion of a β_4 term [Fig. 1(b)] it becomes totally upside down, the value of $\beta_2^{\min}$ remaining unchanged. Also the minimum becomes more localized in the γ direction.

Nucleus ^{192}Os appears most interesting. Figure 2(a) shows a well developed oblate minimum corresponding to the BK Hamiltonian. The effect of $\beta_4=-0.017$, of course with a different Hamiltonian, is seen in Fig. 2(b). This minimum becomes better localized in the β_2 direction but becomes shallower in the γ direction with a clear minimum at $\gamma\approx 45°$. As already mentioned in Sec. III A, we get a second prolate minimum for ^{192}Os with $\beta_4=-0.045$. This is illustrated through the PES of Fig. 2(c). The $\gamma\approx 45°$ minimum of Fig. 2 now shifts to $\gamma\approx 35°$ with the oblate side fully closed with about 150–200 keV curve, and softening on the prolate side. In the self-consistent calculation $S3$ the prolate minimum is about 75 keV higher than the absolute minimum at $\gamma\approx 45°$. We must remember that in the self-consistent calculation $\beta_4^{\min}$ has different values: -0.017 and -0.045, respectively, corresponding to the triaxial and prolate minima. In order to ascertain whether the prolate minimum survives against the zero-point motion we have also calculated PES with such an energy correction (ZPE) (Ref. 10)

$$E=\langle\Phi|H|\Phi\rangle-\mathrm{ZPE}\,,$$
$$\mathrm{ZPE}=\sum_{i=1}^{3}\langle\Phi|\mathcal{J}_i^2|\Phi\rangle/2\mathcal{J}_i \tag{11}$$

with $i=1$, 2, and 3 meaning X, Y, and Z axes. $\mathcal{J}_i$ stands for the ith component of the angular momentum operator and $\mathcal{J}_i$ is the Inglis moment of inertia.[3] As displayed in Fig. 2(d) this leads to an even better developed set of prolate and oblate (instead of $\gamma=45°$) minima, with $\beta_4=-0.045$. However, the equilibrium values of β_2 remain almost unaltered. This is why for other cases PES's are not shown including ZPE.

Next we come to the PES plot of ^{194}Os [Figs. 3(a) and (b)] with $\beta_4=-0.008$ and -0.0344, respectively. For this nucleus also corresponding to larger β_4 value [Fig. 3(b)] there is a second minimum at $\gamma=0$. But this is about 350 keV higher compared to the oblate one. So, according to the energy spacings of Fig. 3(b) this prolate minimum is not clearly seen, except for such a tendency with the convergence of the "E" lines.

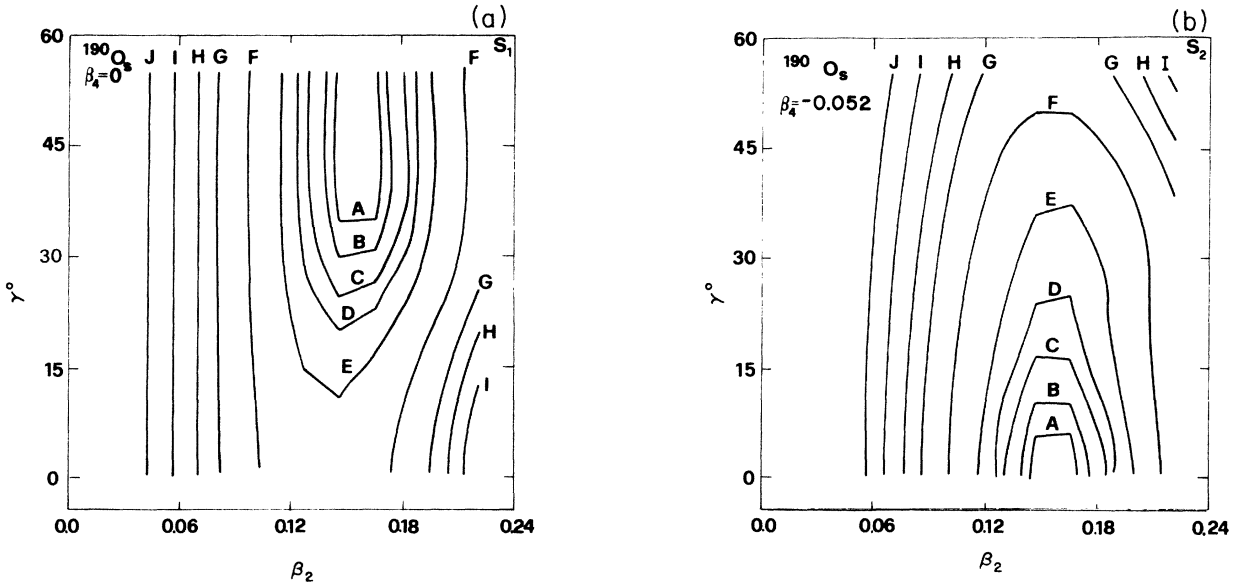

FIG. 1. (a) Potential energy surface (PES) plot in the (β_2,γ) space for ^{190}Os with the BK Hamiltonian designated here as the $S1$ scheme which is indicated on the top right corner of the plot. The equilibrium value of β_4 corresponding to the same scheme is also written. The contour lines labeled A, B, ..., J correspond to energies 20, 50, 100, 150, 250, 500, 800, 1000, 1250, and 1500 keV, respectively. (b) Same as (a) in the $S2$ scheme.

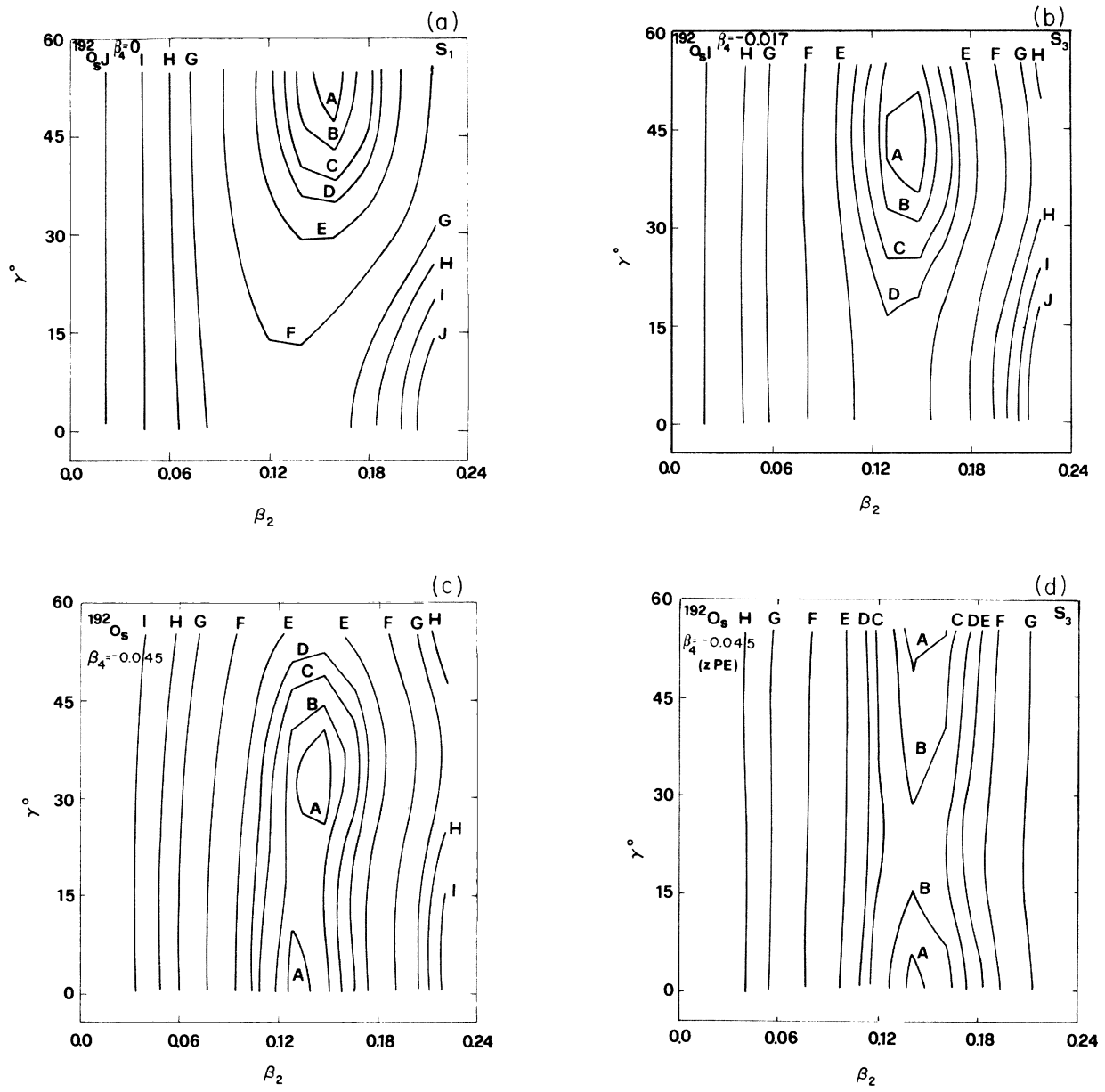

FIG. 2. (a) Same as Fig. 1(a) for ^{192}Os; (b) in the $S3$ scheme; (c) with large β_4 value corresponding to a second minimum at $\gamma=0$; and (d) including zero-point-energy corrections.

Figure 4(a) displays the PES plot of ^{188}Pt with the BK Hamiltonian. No doubt there is a clear minimum at $\gamma=20°$. But this is only a small localization within about the 50 keV region. Then all the lines run almost parallel at each β_2 from $\gamma=0°$ to $\gamma=60°$. On the other hand, in the $S2$ scheme [Fig. 4(b)] we get a well developed prolate minimum with $\beta_4=-0.035$. Thus inclusion of the hexadecapole interaction term in the Hamiltonian seems to have a big effect. Finally, to demonstrate the effect of $\beta_4=-0.013$ and -0.026 corresponding to $S2$ and $S3$, respectively, for ^{190}Pt, we compare Figs. 5(a) and (b). The former shows a minimum at about $\gamma=30°$ with a uniform shallowness towards prolate as well as oblate ends. We know that BK get an oblate minimum (see Table I), whereas Fig. 5(b) shows more softness towards $\gamma=0$.

Thus in Figs. 1–5 we have been able to see a rather subtle influence of the hexadecapole interaction term in the Hamiltonian and the importance of its proper self-consistent treatment. It should also be noted that it affects only the γ degree of freedom, the equilibrium values of β_2 remaining almost unchanged in going from $S1$ to $S3$ for a given nucleus.

C. Nilsson plots

For a deeper analysis of nuclear structure at the s-p level it is always desirable to examine the s-p energy Nilsson plots. We have drawn these diagrams for protons (Fig. 6)

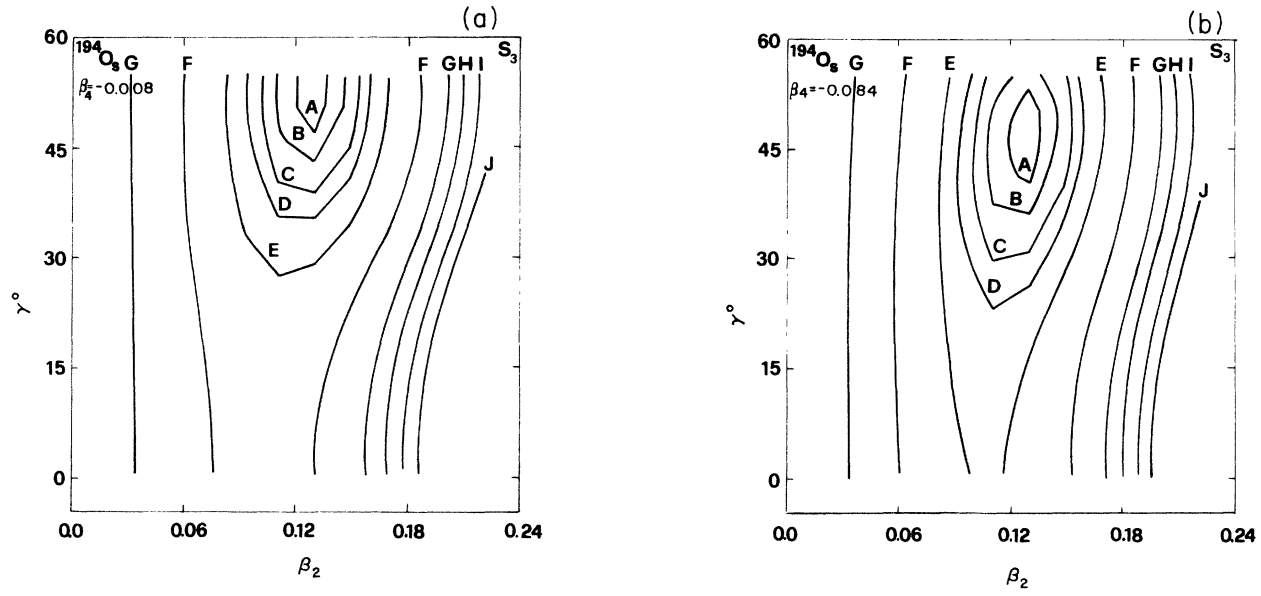

FIG. 3. (a) Same as Fig. 2(a) for ^{194}Os; (b) same as Fig. 2(c) for ^{194}Os.

and neutrons (Fig. 7) using the Hamiltonian (7) with the main motivation to see the effect of a β_4 deformation on the prolate or oblate deformed s-p orbitals. Obviously, the mass dependence comes only through the oscillator frequency $\hbar\omega = 41.2/A^{1/3}$. We have taken $A = 190$. The maximum value of $|\beta_2|$ is taken to be 0.2 only as, for the present, this is the range of our interest. We have two sets of plots with $\beta_4 = 0.0$ and -0.045 for protons as well as neutrons. Considering ^{190}Os as a representative nucleus in this region whose protons fill completely the $h_{11/2}$ subshell and neutrons fill the $i_{13/2}$ subshell at $\beta_2 = 0.0$, we have plotted energy levels approximately within ± 2 MeV about these states. Each curve is labeled by the projection quantum number k of angular momentum j. Solid lines indicate positive parity and dashed ones indicate negative parity states.

Figures 6(a) and (b) display the proton Nilsson diagram with $\beta_4 = 0$ and -0.045, respectively. The Fermi surface (ϵ_F) for $Z = 76$ is indicated by the thick curve in both the figures. The value of $\beta_4 = -0.045$ is rather a strong perturbation for the $\beta_2 \lesssim 0.1$ region. But for us a more useful range is around $|\beta_2| = 0.15$. Comparing carefully Figs. 6(a) and (b) we notice that the levels at the Fermi surface for $Z = 76$ do get rearranged in the presence of β_4,

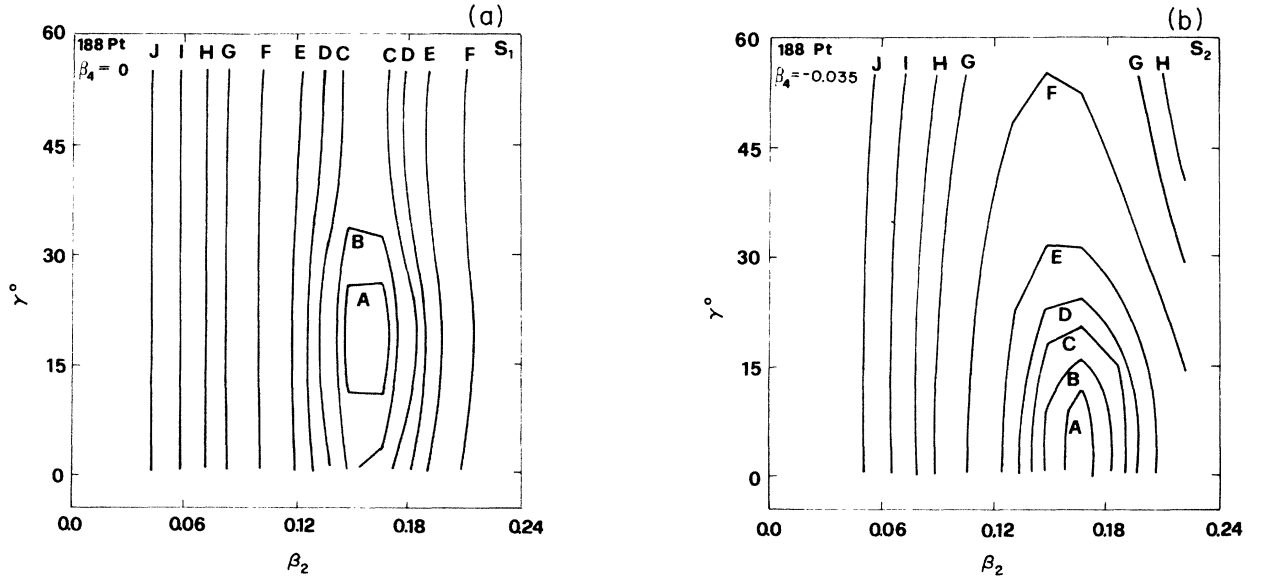

FIG. 4. (a) Same as Fig. 1(a) for ^{188}Pt; (b) same as (a) in the $S2$ scheme.

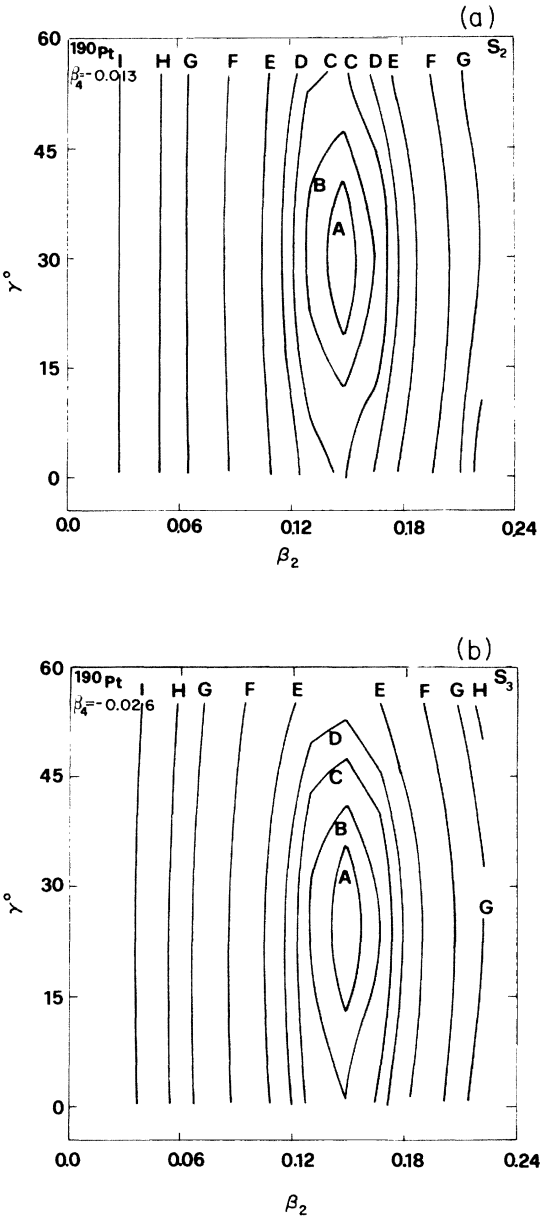

FIG. 5. (a) Same as Fig. 4(b) for ^{190}Pt; (b) same as (a) in the $S3$ scheme.

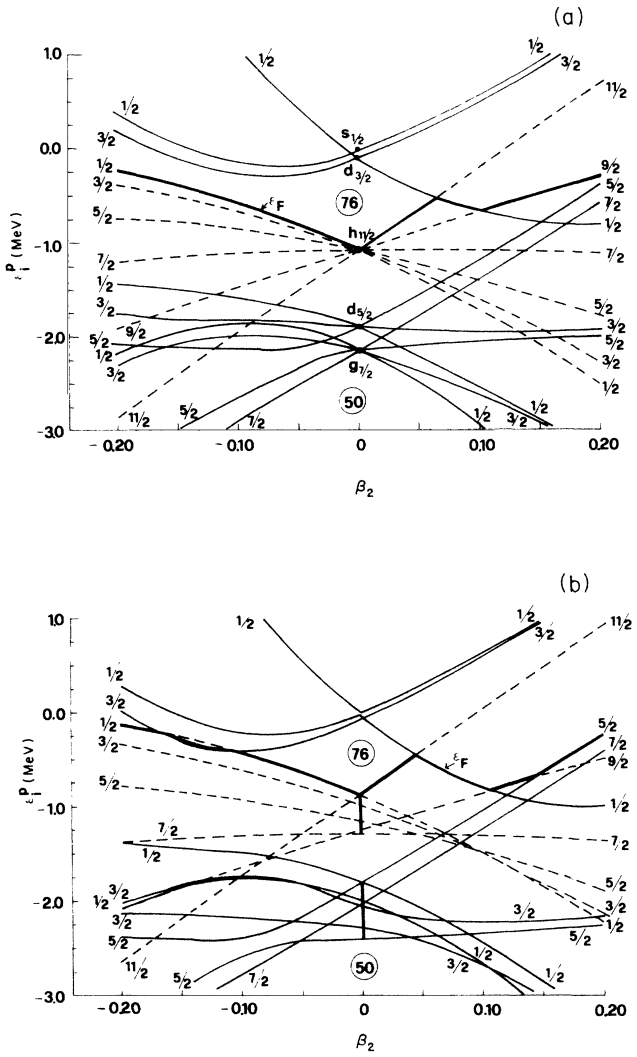

FIG. 6. (a) Single particle energy Nilsson plot for protons corresponding to mass number $A=190$ with $\beta_4=0.0$. The Fermi surface for $Z=76$ is indicated by the thick curve. Solid lines imply orbitals with positive parity and dashed ones with negative parity. (b) Same as (a) with $\beta_4=-0.045$.

whereas for $Z=78$ (Pt) it does not happen. Particularly, if we look at Table I for the equilibrium values of β_4 for the Pt isotopes, the largest value of β_4 is -0.035. So, for such or smaller β_4 values the $Z=78$ Fermi surface should indeed remain unaffected. On the other hand, for ^{188}Os we need $\beta_4=-0.055$.

Similarly, we have Figs. 7(a) and (b) for neutrons. We observe that on prolate as well as oblate sides for $|\beta_2|=0.15$–0.2 there is a considerable rearrangement of the orbitals near the $N=114$ Fermi surface. It is important to realize that on the oblate side small k, small l negative parity orbitals are interwoven with small k, large l positive parity orbitals. On the other hand, on the prolate side important orbitals come from large l $h_{9/2}$ and $i_{13/2}$ states with large k values. To give a better picture of how some orbitals near ϵ_F get reordered in the presence of β_4 we have listed in Table II five neutron orbitals giving their energies and wave function components C_{jk} [Eq. (4)]. From the sign of the parity indicated over the k values the l values can be ascertained for the basis space used here. There are four sets [(a)–(d)] corresponding to $\beta_2=0.16$, $\gamma=0$, 60°, and $\beta_4=0$, -0.045. Let us mention about some notable changes. For example, in the first part of Table II $\frac{7}{2}^-$ is about 500 keV below the Fermi surface (underlined) and in the second part of Table II it is only about 80 keV below ϵ_F. Another level $\frac{1}{2}^+$ $(i_{13/2})$ is only about 225 keV above ϵ_F in the third part of Table II but in the presence of β_4 it is pushed up by about 560 keV.

Of course, the net macroscopic effect like the equilibri-

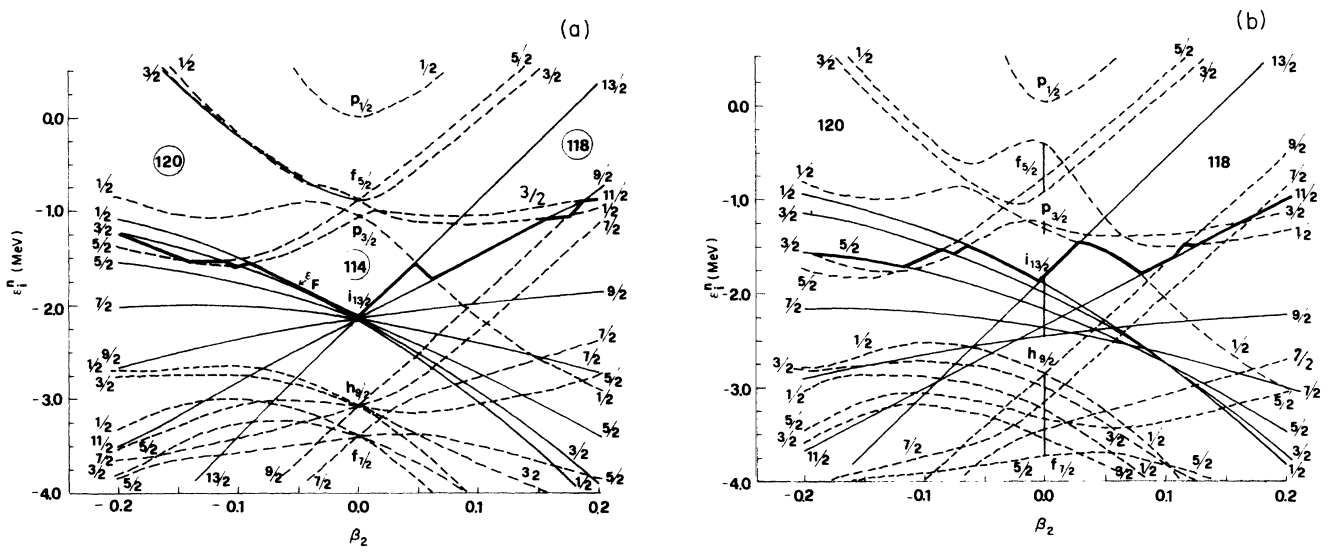

FIG. 7. (a) Same as Fig. 6(a) for neutrons. The Fermi surface for $N=114$ is indicated by a thick curve. (b) Same as (a) with $\beta_4=-0.045$.

TABLE II. Five Nilsson orbitals for neutrons near the $N=114$ Fermi surface for prolate and oblate shapes with and without β_4 corresponding to a realistic value of $\beta_2=0.16$ in the Os-Pt region are listed: (a) $\gamma=0$, $\beta_4=0$; (b) $\gamma=0$, $\beta_4=-0.045$; (c) $\gamma=180°$, $\beta_4=0$; (d) $\gamma=180°$, $\beta_4=-0.045$. The Fermi surface is underlined. j and its projection quantum number k (labels on C_{jk}) are listed. The parity is indicated by the symbol π.

ϵ_i^n (MeV)	k^π	j $\frac{1}{2}$	$\frac{3}{2}$	$\frac{5}{2}$	$\frac{7}{2}$	$\frac{9}{2}$	$\frac{11}{2}$	$\frac{13}{2}$
(a)								
−0.969	$\frac{3}{2}^-$		0.370	−0.836	0.265	−0.304	−0.044	
−1.084	$\frac{1}{2}^-$	0.037	0.693	0.588	0.327	0.250	−0.048	
<u>−1.085</u>	$\frac{11}{2}^+$						−0.040	0.999
−1.248	$\frac{9}{2}^-$						−0.999	−0.051
−1.589	$\frac{7}{2}^-$				−0.950	−0.302	−0.074	
(b)								
−0.992	$\frac{9}{2}^-$					0.997	0.071	
<u>−1.258</u>	$\frac{3}{2}^-$		−0.343	0.829	−0.256	0.356	−0.050	
−1.277	$\frac{11}{2}^+$						−0.058	−0.998
−1.337	$\frac{7}{2}^-$				−0.957	−0.271	−0.107	
−1.419	$\frac{1}{2}^-$	−0.014	0.640	−0.634	0.332	−0.227	0.042	
(c)								
−1.222	$\frac{1}{2}^+$	0.008	0.001	0.046	0.003	0.232	0.006	0.972
−1.350	$\frac{3}{2}^+$		−0.005	0.041	−0.009	0.224	−0.019	0.974
<u>−1.448</u>	$\frac{3}{2}^-$		−0.640	−0.358	0.547	0.393	−0.097	
−1.503	$\frac{5}{2}^-$			−0.762	0.318	0.559	−0.073	
−1.609	$\frac{5}{2}^+$			0.030	0.012	0.206	0.031	0.977
(d)								
−1.069	$\frac{1}{2}^+$	0.011	0.001	0.060	0.002	0.262	0.010	0.962
−1.257	$\frac{3}{2}^+$		−0.002	−0.044	0.005	−0.243	0.028	−0.969
<u>−1.629</u>	$\frac{5}{2}^+$			−0.019	−0.005	−0.200	−0.045	−0.979
−1.725	$\frac{3}{2}^-$		0.717	0.302	−0.445	−0.438	0.070	
−1.818	$\frac{5}{2}^-$			0.842	−0.257	−0.468	0.080	

um value of β_2 or γ is related in a very complex manner to the sum of the single-particle expectation values of the multipole operators. Through Figs. 6 and 7 and Table II we can get at least an appreciation and some understanding of how some orbitals are affected in the presence of a hexadecapole deformation.

IV. CONCLUSIONS

In a microscopic many-body approach we are able to get a structural phase transition in the Os-Pt region which seems in conformity with the recent empirical analysis of Casten *et al.*[2] Baktash *et al.*[40] have recently concluded that γ-soft models show an overall better agreement with the systematics of static quadrupole moments in this region. Looking at energies as a function of γ in Figs. 1–5 our results also are γ soft.

To understand the behavior of the Os isotopes inclusion of a β_4 term like Eq. (6) or (7) should be enough as most important are the prolate ($+\beta_2$, $\gamma=0$) and oblate ($-\beta_2$, $\gamma=0$) shapes, the transition being almost abrupt at $A=192-194$.

However, to get a smooth shape transition in the Pt isotopes a fully self-consistent treatment of the hexadecapole term in the Hamiltonian (1) is essential, and of course this is the right thing to do.

Thus from the present investigations it emerges that (i) Os are prolate for $A \leq 190$, oblate for $A \geq 194$, and at $A=192$ prolate and oblate shapes compete with each other. (ii) Pt are prolate for $A \leq 186$, oblate for $A \geq 194$, and triaxial but not γ rigid for $A=188-192$.

ACKNOWLEDGMENTS

Some preliminary exploration of this topic was done in collaboration with L. Satpathy and R. Sahu. This work in its present framework has been carried out totally at the ICTP during a visit by the author. Kind cooperation of the computer staff is gratefully acknowledged. He also wishes to thank the International Atomic Energy Agency and UNESCO for hospitality at the International Centre for Theoretical Physics, Trieste.

*On leave from Institute of Physics, Bhubaneswar-751005, India.

[1]R. F. Casten and J. A. Cizewski, Nucl. Phys. **A309**, 477 (1978).
[2]P. D. Bond, R. F. Casten, D. D. Warner, and D. Horn, Phys. Lett. **130B**, 167 (1983).
[3]M. Baranger and K. Kumar, Nucl. Phys. **A110**, 490 (1968); K. Kumar and M. Baranger, *ibid.* **A110**, 529 (1968).
[4]K. Kumar and M. Baranger, Nucl. Phys. **A122**, 273 (1968).
[5]K. J. Weeks and T. Tamura, Phys. Rev. Lett. **44**, 533 (1980).
[6]M. Girod and B. Grammaticos, Phys. Rev. Lett. **40**, 361 (1978).
[7]U. Götz, H. C. Pauli, K. Alder, and K. Junker, Nucl. Phys. **A192**, 1 (1972).
[8]I. Ragnarsson, A. Sobiczewski, R. K. Sheline, S. E. Larsson, and B. Nerlo-Pomorska, Nucl. Phys. **A233**, 329 (1974).
[9]G. A. Leander, P. Arve, T. Bengtsson, I. Ragnarsson, and J. Y. Zhang, Nucl. Phys. **A400**, 97c (1983).
[10]R. Sahu, M. Satpathy, A. Ansari, and L. Satpathy, Phys. Rev. C **19**, 511 (1979).
[11]L. Wilets and M. Jean, Phys. Rev. **102**, 788 (1956).
[12]A. S. Davydov and G. F. Filippov, Nucl. Phys. **8**, 237 (1958).
[13]H. Toki and A. Faessler, Z. Phys. A **276**, 35 (1976).
[14]I. Y. Lee, D. Cline, P. A. Butler, R. M. Diamond, J. O. Newton, R. S. Simon, and F. S. Stephens, Phys. Rev. Lett. **39**, 684 (1977).
[15]F. Todd Baker, Nucl. Phys. **A331**, 39 (1979).
[16]R. Sahu, Phys. Rev. C **29**, 1486 (1984).
[17]J. A. Cizewski, R. F. Casten, G. J. Smith, M. L. Stelts, W. R. Kane, H. G. Börner, and W. F. Davidson, Phys. Rev. Lett. **40**, 167 (1978).
[18]F. T. Baker, M. A. Grimm, Jr., A. Scott, R. C. Styles, T. H. Kruse, K. Jones, and R. Suchannek, Nucl. Phys. **A371**, 68 (1981).
[19]A. E. L. Dieperink and R. Bijker, Phys. Lett **116B**, 77 (1982).
[20]A. E. L. Dieperink, Comments Nucl. Part. Phys. **14**, 25 (1985).
[21]K. Heyde, P. van Isacker, M. Waroquier, and J. Mareau, Phys. Rev. C **29**, 1420 (1984).
[22]R. F. Casten and P. von Brentano, Phys. Lett. **152B**, 22 (1985).
[23]P. Federman and S. Pittel, Phys. Lett. **69B**, 385 (1977).
[24]S. C. K. Nair, A. Ansari, and L. Satpathy, Phys. Lett. **71B**, 257 (1977).
[25]R. F. Casten, Phys. Rev. Lett. **54**, 1991 (1985).
[26]A. E. Stuchbery, I. Morrison, and H. H. Bolotin, Phys. Lett. **139B**, 259 (1984).
[27]H. H. Bolotin, C. E. Doron, I. Morrison, L. D. Wood, and H. Yamada, Z. Phys. A **320**, 669 (1985).
[28]M. Brack, J. Damgaard, A. S. Jensen, H. C. Pauli, V. M. Strutinsky, and C. Y. Wong, Rev. Mod. Phys. **44**, 320 (1972).
[29]F. T. Baker, T. H. Kruse, W. Hartwig, I. Y. Lee, and J. X. Saladin, Nucl. Phys. **A258**, 43 (1976).
[30]A. Ansari, O. Civitarese, and A. Faessler, Nucl. Phys. **A334**, 93 (1980).
[31]W. Nazarewicz and P. Rozmej, Nucl. Phys. **A369**, 396 (1981).
[32]Th. J. Köpel, A. Faessler, and U. Götz, Nucl. Phys. **A403**, 263 (1983).
[33]T. Bengtsson and I. Ragnarsson, Nucl. Phys. **A436**, 14 (1985).
[34]B. Fogelberg, Nucl. Phys. **A197**, 497 (1972).
[35]H. Helppi, A. Pakkanen, and J. Hattula, Nucl. Phys. **A223**, 13 (1974).
[36]R. F. Casten, A. I. Namenson, W. F. Davidson, D. D. Warner, and H. G. Börner, Phys. Lett. **76B**, 280 (1978).
[37]J. F. W. Jansen and H. Pauw, Nucl. Phys. **A94**, 235 (1967).
[38]M. Finger *et al.*, Nucl. Phys. **A188**, 369 (1972).
[39]S. W. Yates, J. C. Cunnane, R. Hochel, and P. J. Daly, Nucl. Phys. **A222**, 301 (1974).
[40]C. Baktash, J. X. Saladin, J. J. O'Brien, and J. G. Alessi, Phys. Rev. C **22**, 2383 (1980).